Model Validation for Propulsion – On the TFNS and LES Subgrid Models for a Bluff Body Stabilized Flame

Thomas Wey

NASA Glenn Research Center, Cleveland OH 44135 USA

Outline of Paper

- Overview of the validation case.
- Overview of the code used for model validation: a releasable edition of the National Combustion Code (also known as OpenNCC).
- The results of a non-reacting case.
- The results of a reacting case.

Workshop Case

Computational domain and boundaries for the Volvo test case

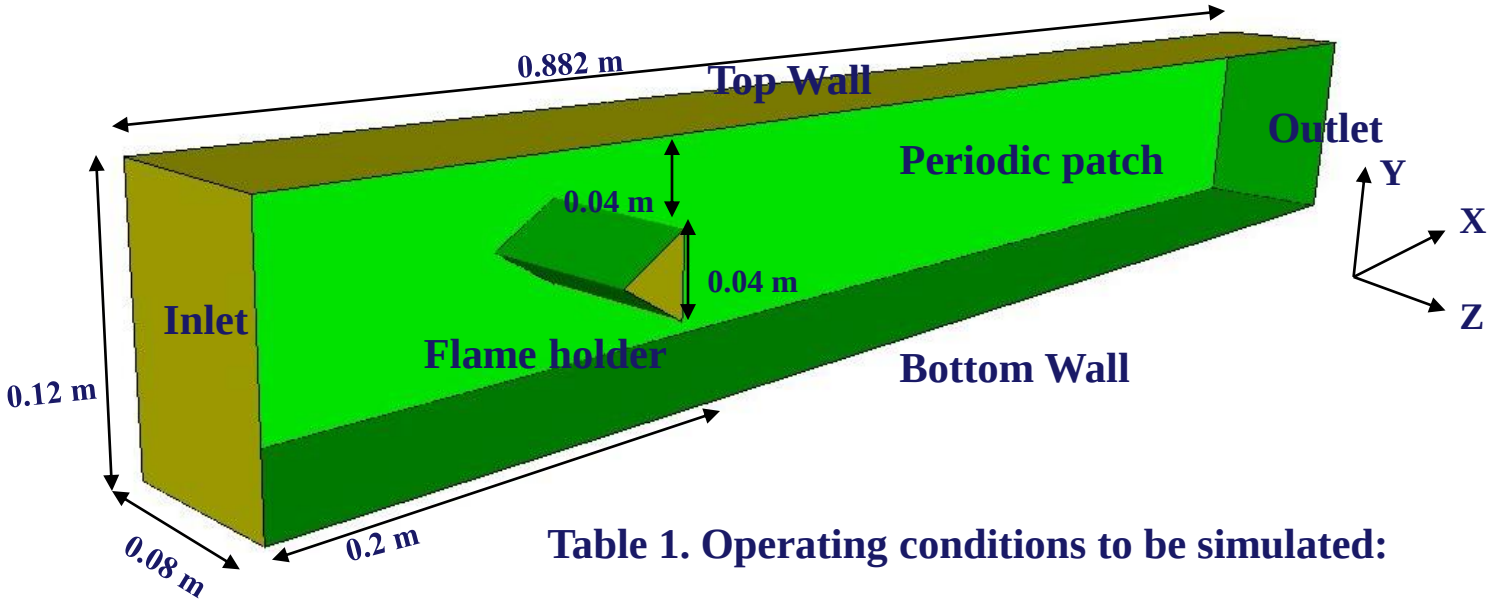

Table 1. Operating conditions to be simulated:

Fuel	Propane
Oxidizer	Air
Mass Flow Rate	0.2083 kg/s
Inlet Temperature	288.2 K
Premixed Equivalence Ratio	0.65

Releasable edition of the NCC

- **Gaseous solver is a pre-conditioning enabled polyhedral finite–volume code. CFD cells can have an arbitrary number of faces and faces can have an arbitrary number of points. Spray solver is based on a Lagrangian scheme.**
- **A second order accurate central or upwind scheme is used for spatial discretization of the Euler fluxes. A second order accurate central scheme is used for discretization of the Laplacian terms.**
- **Temporal integration options: (1) non-iterative second order MacCormack scheme; (2) dual-time 2-stage modified MacCormack scheme; (3) dual-time 3-4-5-stage Runge-Kutta scheme.**

Releasable edition of the NCC

- **Subgrid models for mixing and combustion, Eulerian probability density function (EUPDF) and linear-eddy mixing (LEM) are available.**
- **Four major differences between turbulence models in terms of coding are listed below**

Turbulence Model	Turbulence Stresses	Eddy Viscosity	K-Destruction Term	Coefficients
TFNS	Quadratic and Cubic	$C_\mu \rho K^2/\varepsilon$	$\rho\varepsilon$	RCP: Prescribed
K - LES	Linear	$C_v \rho K^{0.5} \Delta$	$C_\varepsilon \rho (K)^{1.5}/\Delta$	C_v, C_ε: Prescribed or computed by LDKM scheme
LES	Linear	$(C_s\Delta)^2 \rho \lvert S \rvert$	N/A	C_s, Prescribed
TFNS/LES	Quadratic and Cubic	$\mathrm{Min}(C_\mu \rho K^2/\varepsilon, (C_s\Delta)^2 \rho \lvert S \rvert)$	$\mathrm{Max}(\rho\varepsilon, C_\varepsilon \rho (K)^{1.5}/\Delta)$	RCP: Prescribed C_ε, C_s: Prescribed

Non-Reacting case

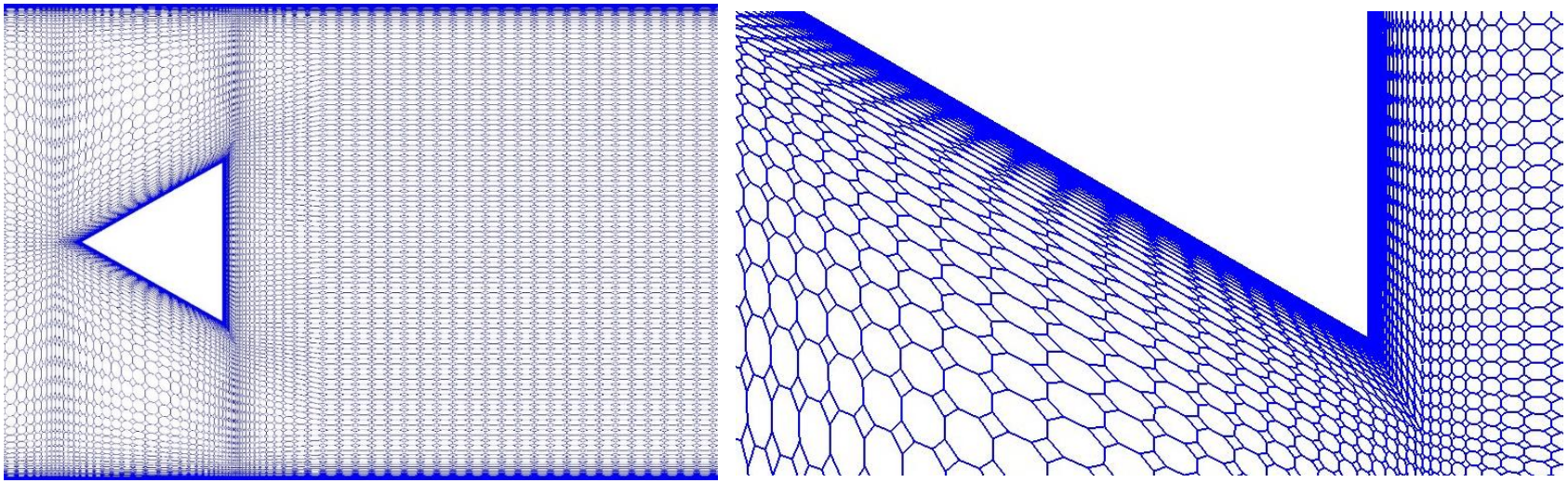

1,667,518 polyhedrons are derived from workshop-provided 4mm-800k hexahedrons by a truncation technique. Its face-to-element ratio is increased from 3.06 to 5.43.

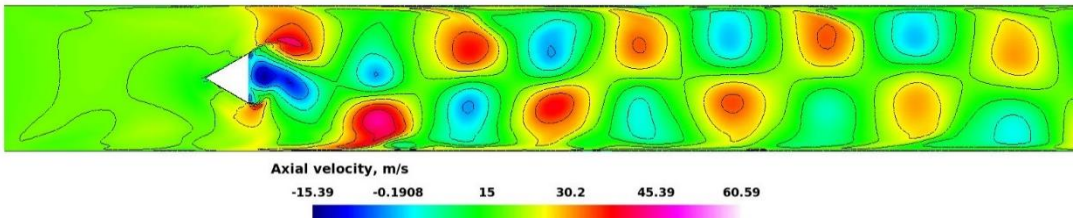

TFNS
Inlet flow rate = 0.2083 kg/s
Back pressure = 100000 Pa

Instantaneous axial velocity contours for the non-reacting case.

Non-Reacting case

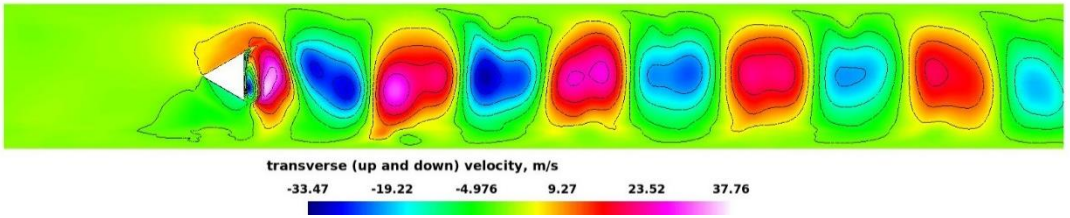

TFNS
Inlet flow rate = 0.2083 kg/s
Back pressure = 100000 Pa

Instantaneous Y-velocity contours for the non-reacting case.

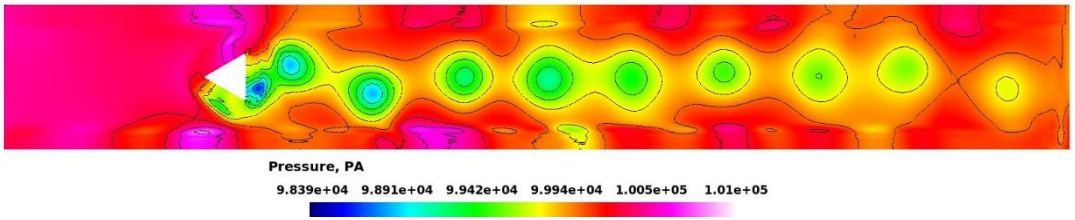

TFNS
Inlet flow rate = 0.2083 kg/s
Back pressure = 100000 Pa

Instantaneous pressure contours for the non-reacting case.

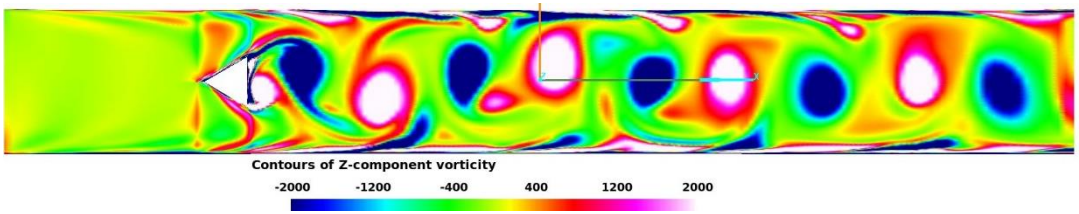

TFNS
Inlet flow rate = 0.2083 kg/s
Back pressure = 100000 Pa

Instantaneous Z-vorticity contours for the non-reacting case.

Non-Reacting case

Mean values of variables are ensemble averages of unsteady values of variables. They are computed in the code and saved to the disk.

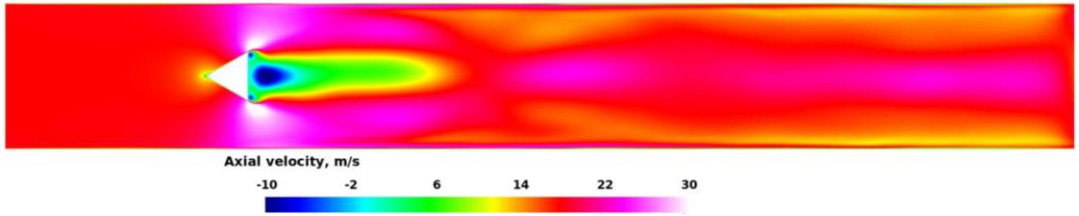

Mean axial velocity contours in mid-plane for the non-reacting case

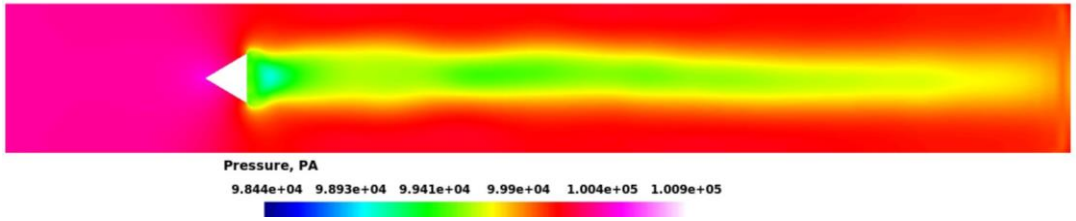

Mean pressure contours in mid-plane for the non-reacting case

Non-Reacting case

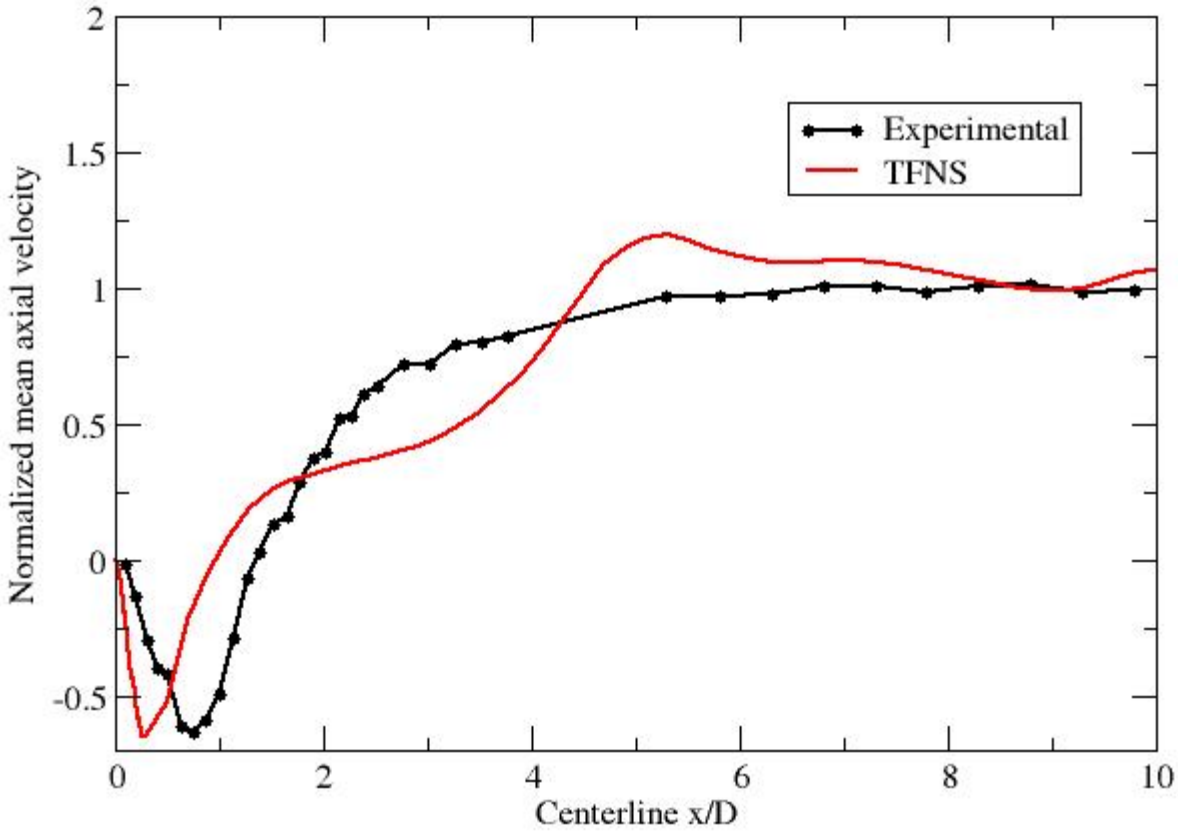

Centerline profiles for the normalized mean axial velocity on a 1.6m polyhedral grid for non-reacting case from TFNS option (i.e. u_x/(16.6 m/s))

Non-Reacting case

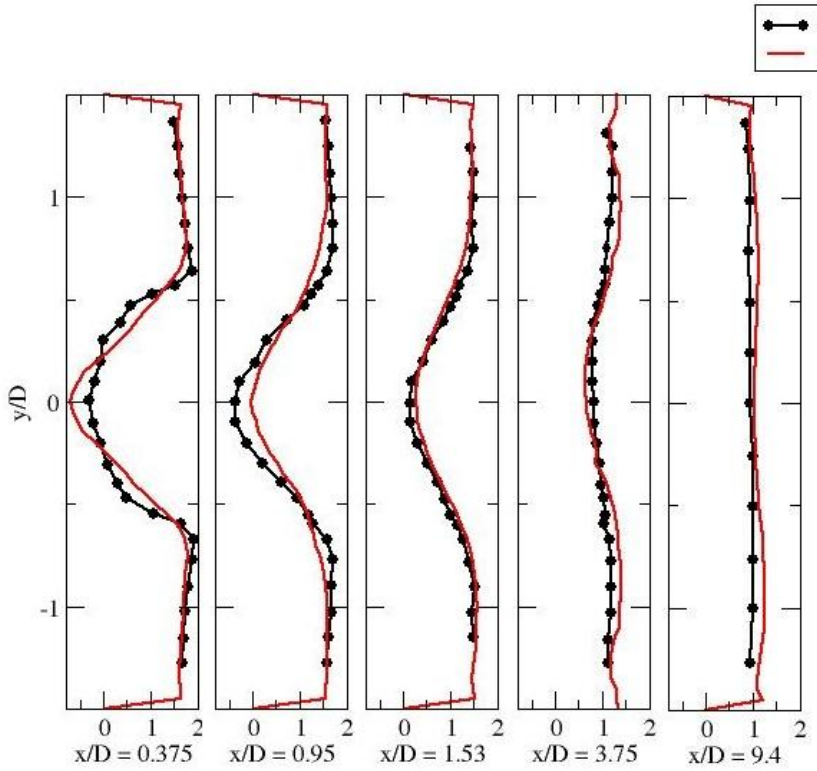

Transverse profiles of normalized mean axial velocity at different axial locations.

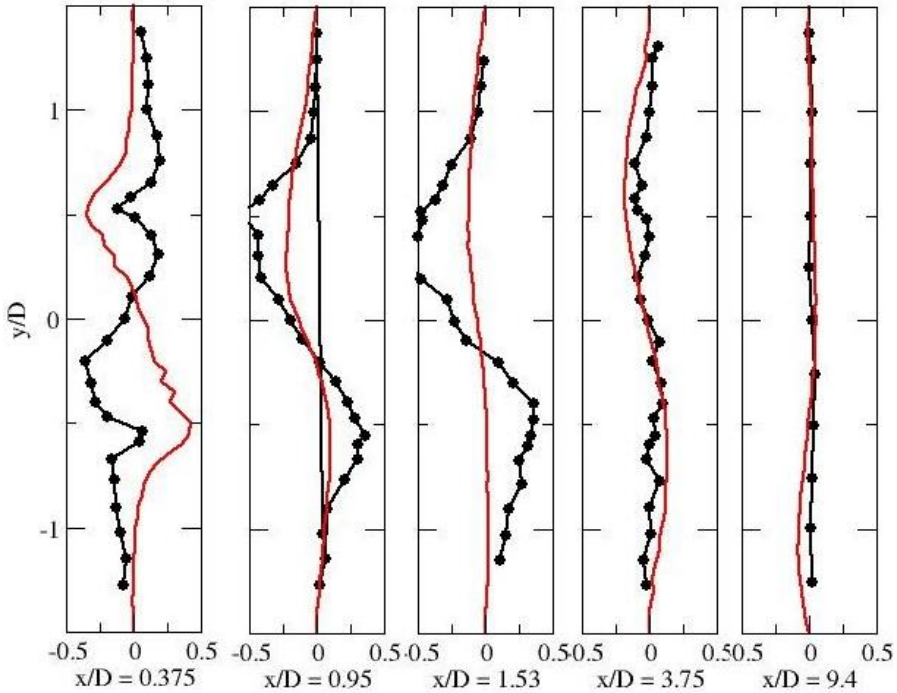

Transverse profiles of normalized mean Y-velocity at different axial locations

Temporal fluctuations of variables sets for the non-reacting case are not post-processed due to lack of disk space to store unsteady data.

Reacting case

From the previous slides, it is speculated that the reason of the poor agreement between the numerical results and the experimental data is due to the type mesh used in the non-reacting case, hence the *original 800k all hexahedral mesh* from the workshop is used for the reacting case.

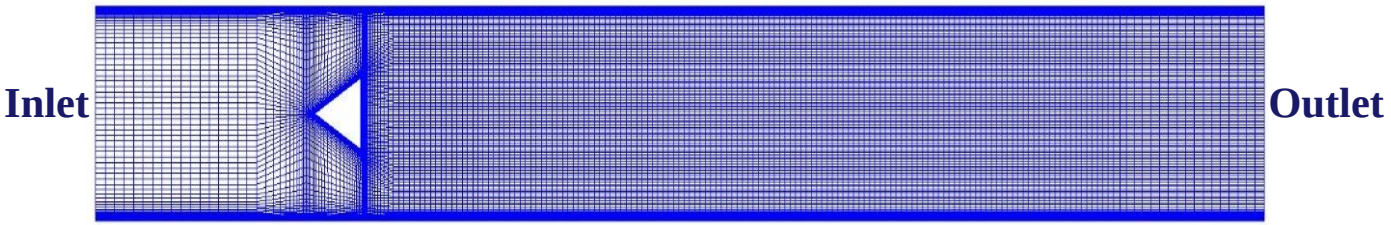

Fuel	C3H8
Air	O2 and N2
Bulk inlet velocity	17.3 m/s
Inlet Temperature	288.2 K
Premixed equivalence Ratio	0.65
Exit static pressure	100000 Pa

Reaction Mechanism for Reacting case

The mechanism is quite similar to the one recommended by the workshop. The changes are: (1) The stoichiometric coefficients of the reaction kinetics have been multiplied by 2 to be integers because the code only accepts integer stoichiometric coefficients and thus the pre-exponential factor of reaction constants have been divided by 2. (2) The global modifiers have been applied to the second reaction in order to keep *exponential factors of concentrations the same as those of workshop mechanism.*

REACTIONS					cgs	Cal/mol
2 C3H8	+ 7 O2	= >	6 CO	+8 H2O	1.0E+12	*33000*
GLO / C3H8	*0.9028/*					
GLO / O2	*0.6855/*					
2 CO	+ 1 O2	< = >	2 CO2		2.25E+10	*12000*
GLO / CO	*1.0/*					
GLO /O2	*0.5/*					

Reacting case

Two turbulence models were selected for simulations, (a) time-filtered Navier-Stokes (denoted TFNS) approach, (b) sub-grid kinetic energy based LES approach, denoted K-LES. The resolution control parameter (RCP) in TFNS is set to 0.5. The coefficient, C_v, of K-LES eddy viscosity is 0.067 initially and the coefficient, C_ε, of the destruction term of kinetic energy transport equation is 0.916 initially. The option to compute them (C_v and C_ε) using the "localized dynamic kinetic energy model" (LDKM) was turned on later.

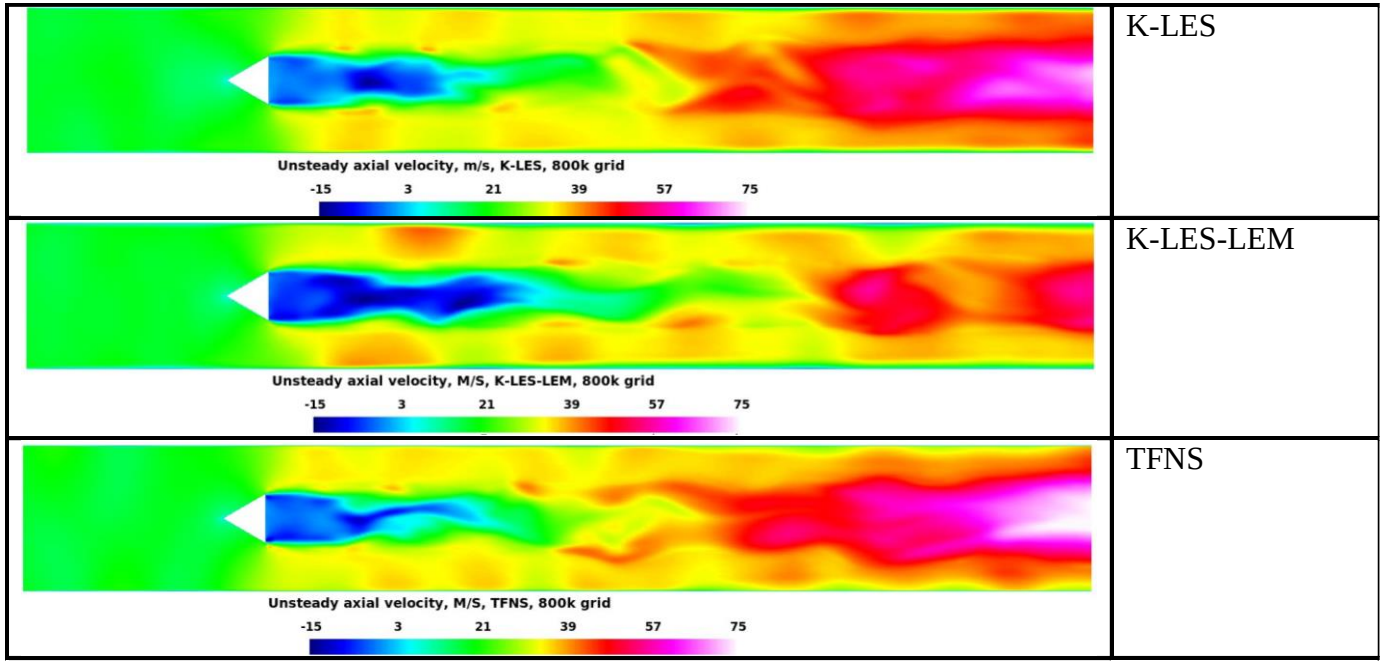

Instantaneous axial velocity (M/S) contours of a two-step global kinetic reaction model for propane

Reacting case

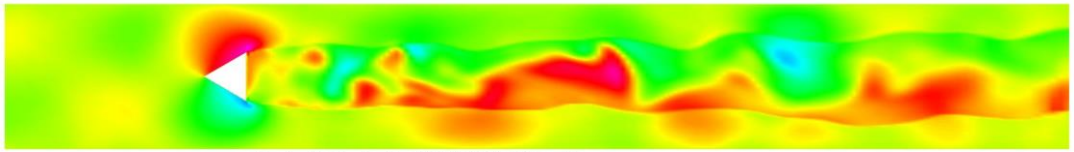	K-LES
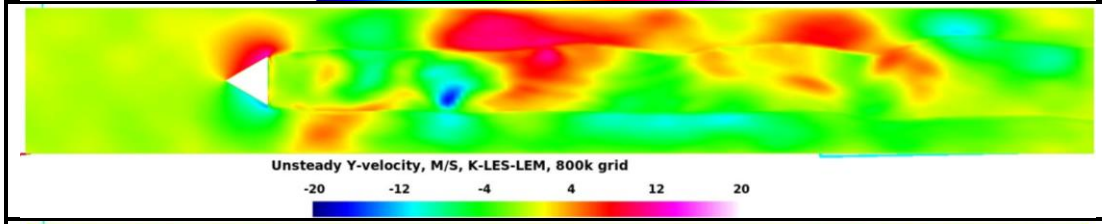	K-LES-LEM
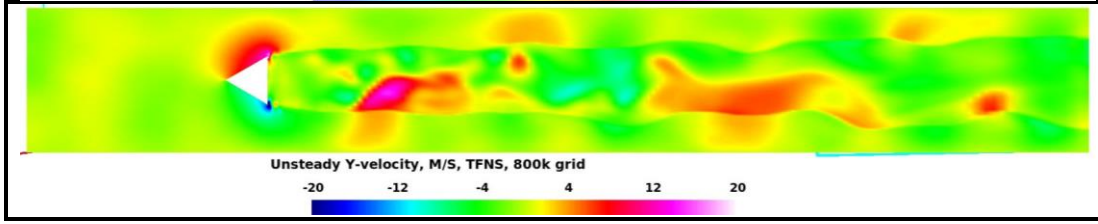	TFNS

Instantaneous Y-velocity (M/S) contours of a two-step global kinetic reaction model for propane

Reacting case

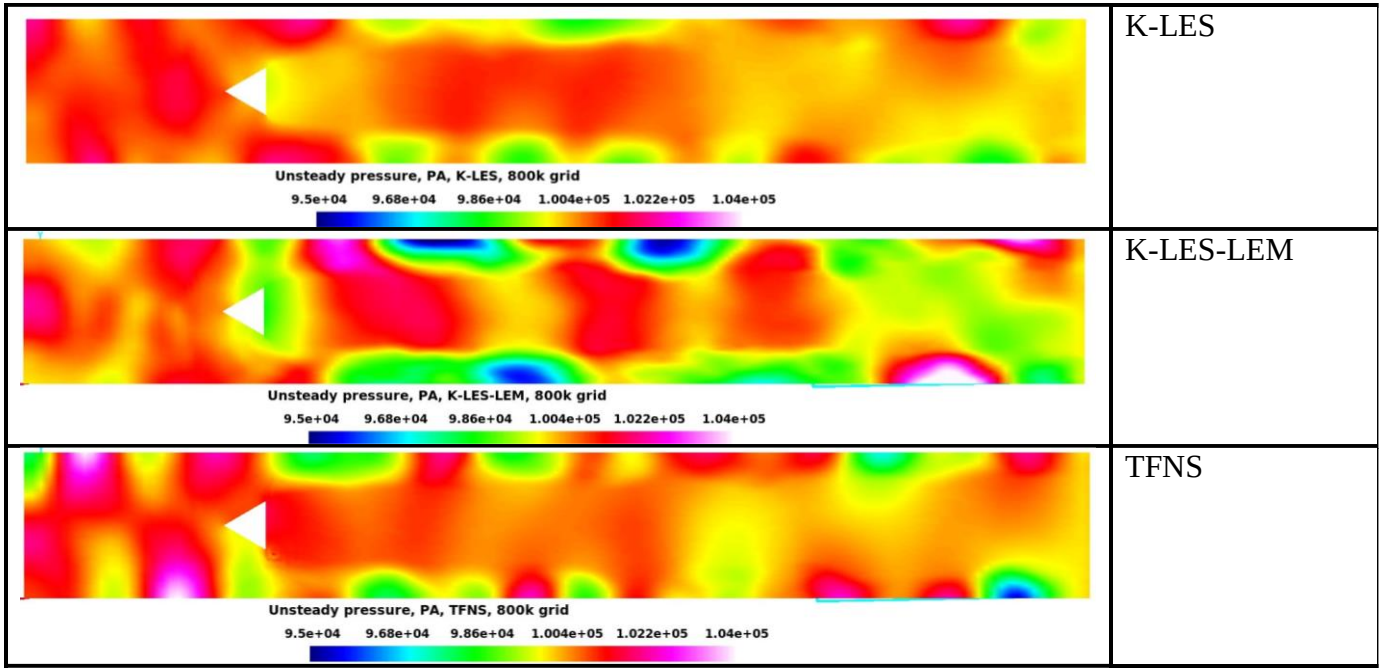

Instantaneous pressure (Pa) contours of a two-step global kinetic reaction model for propane

Reacting case

Because a two-step global kinetic reaction model for C3H8 is used, the influence of the mass fraction of CO is small, the geometry of the flame is less wavy.

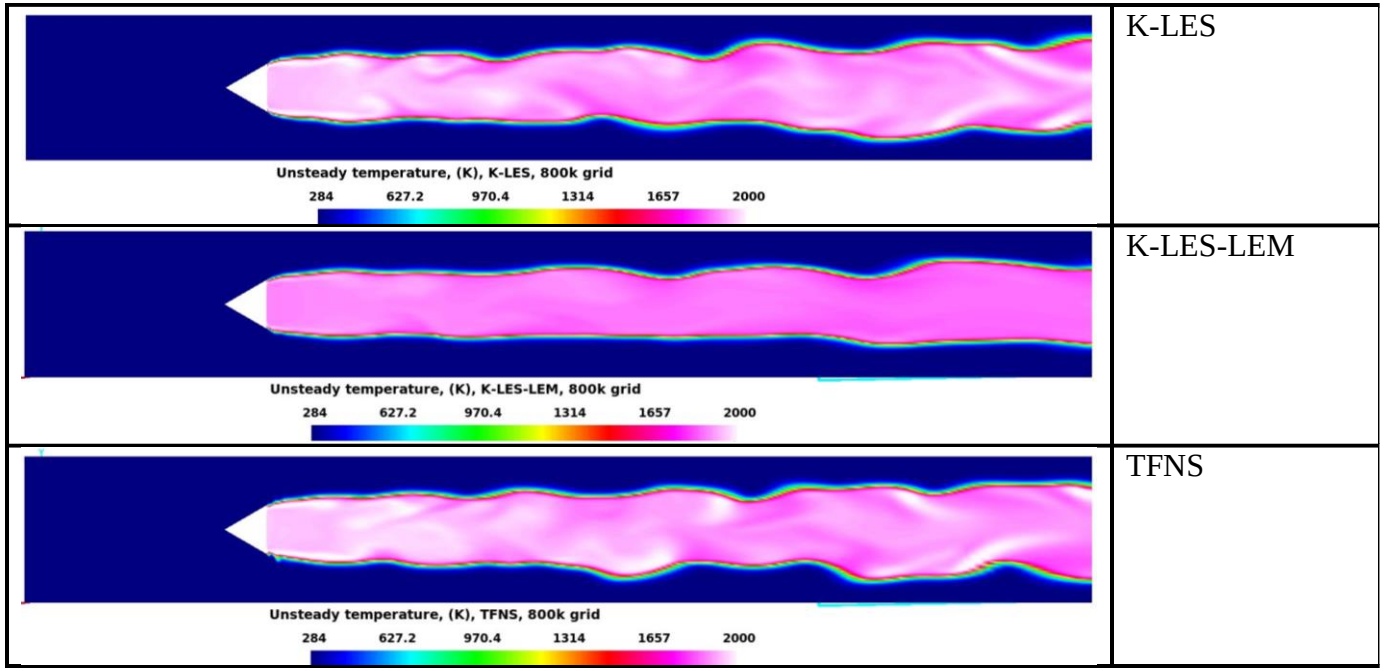

Instantaneous temperature (K) contours of a two-step global kinetic reaction model for propane

Reacting case

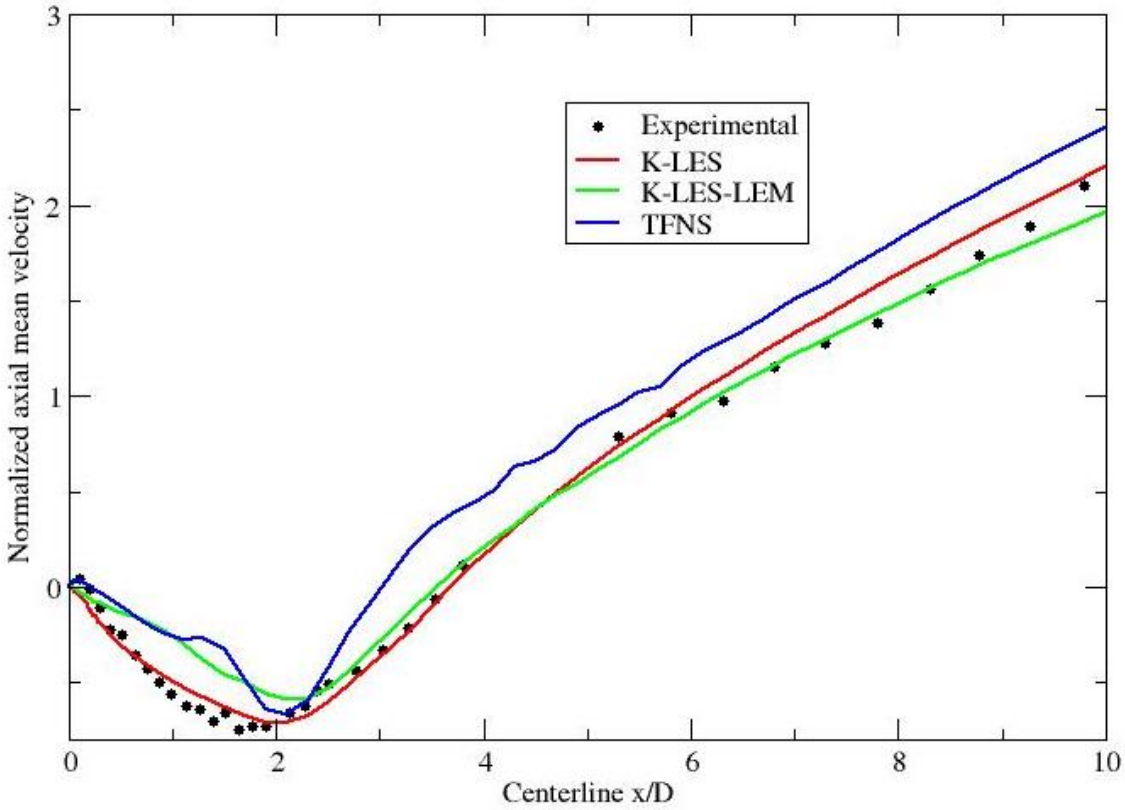

Centerline profiles for the normalized mean axial velocity on the 800k grid for reacting solutions from K-LES, K-LES-LEM and TFNS options.

Reacting case

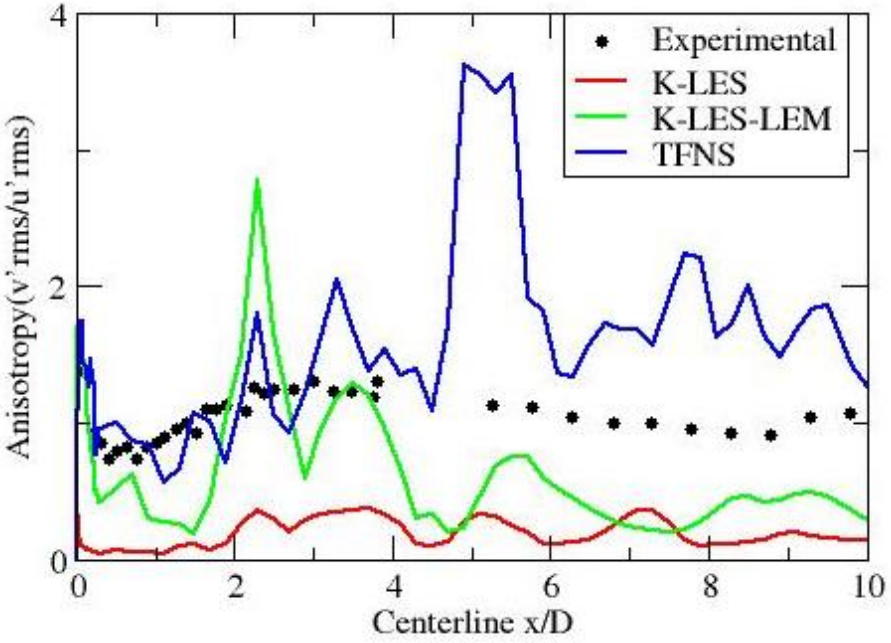

Centerline profiles for the normalized fluctuation level of anisotropy

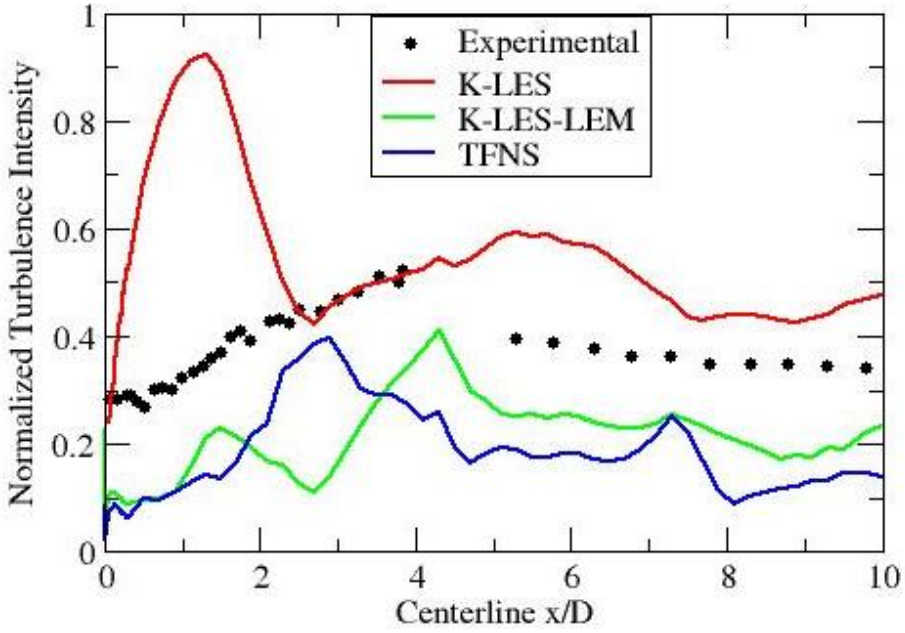

Centerline profiles for the normalized fluctuation level of turbulence intensity

All temporal fluctuations of variables for the reacting case are post-processed with limited number of sets of solutions stored due to lack of disk space.

Reacting case

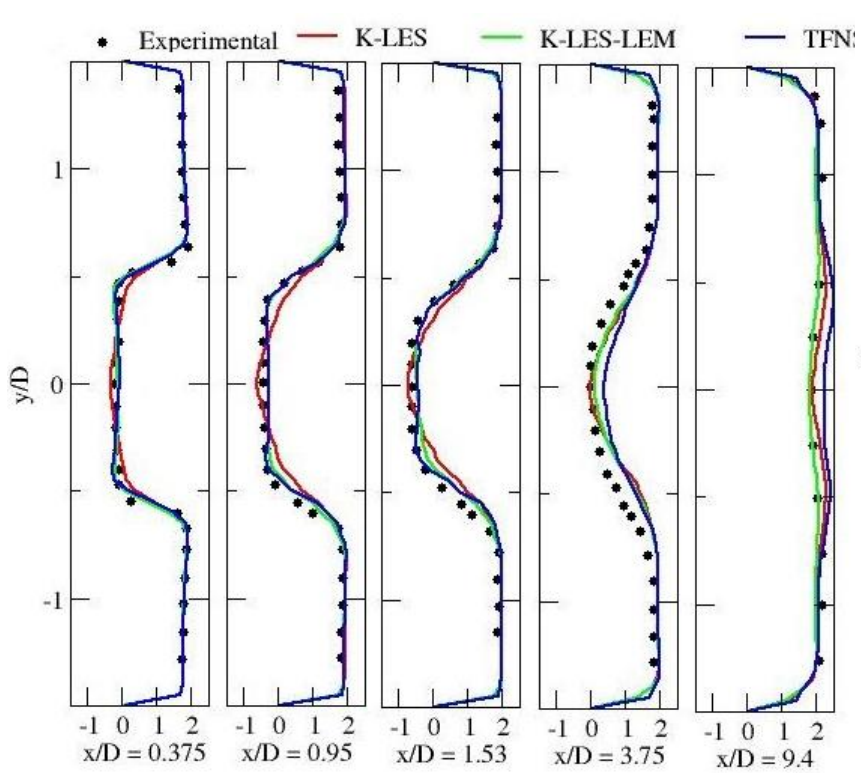

Transverse profiles of normalized mean axial velocity at different axial locations.

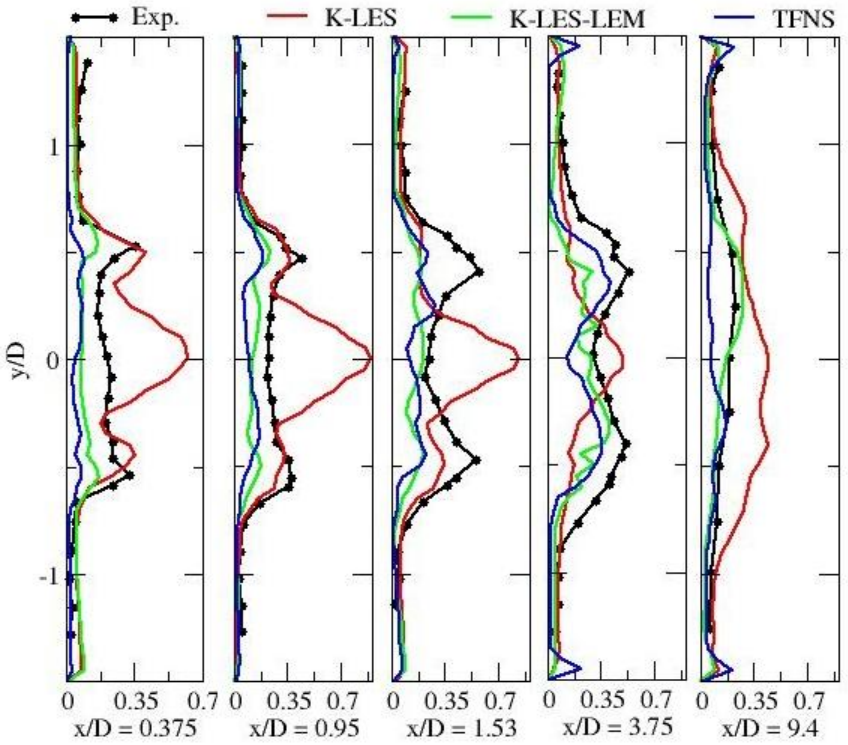

Transverse profiles of normalized axial RMS velocity at different axial locations.

Reacting case

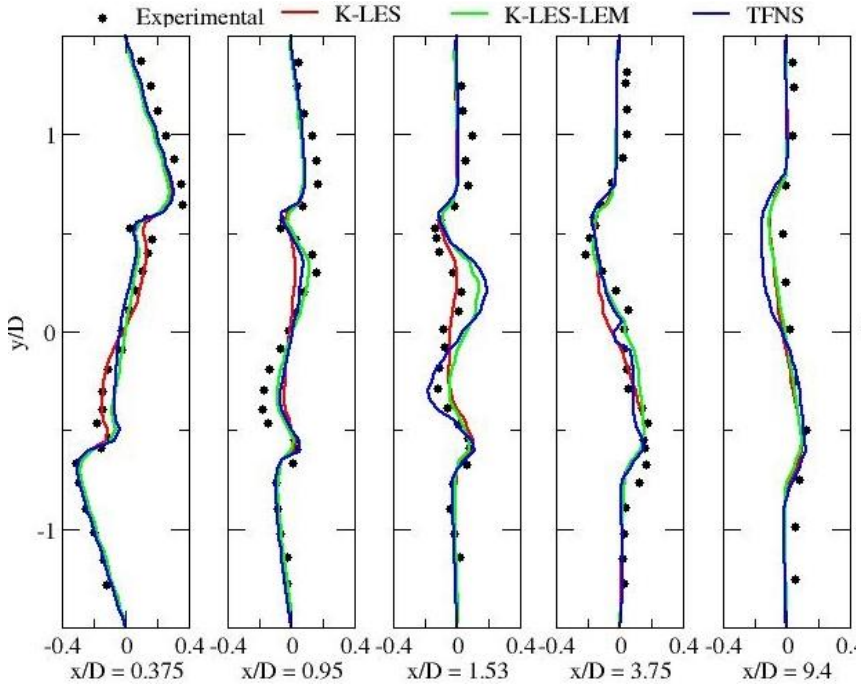

Transverse profiles of normalized mean Y-velocity at different axial locations

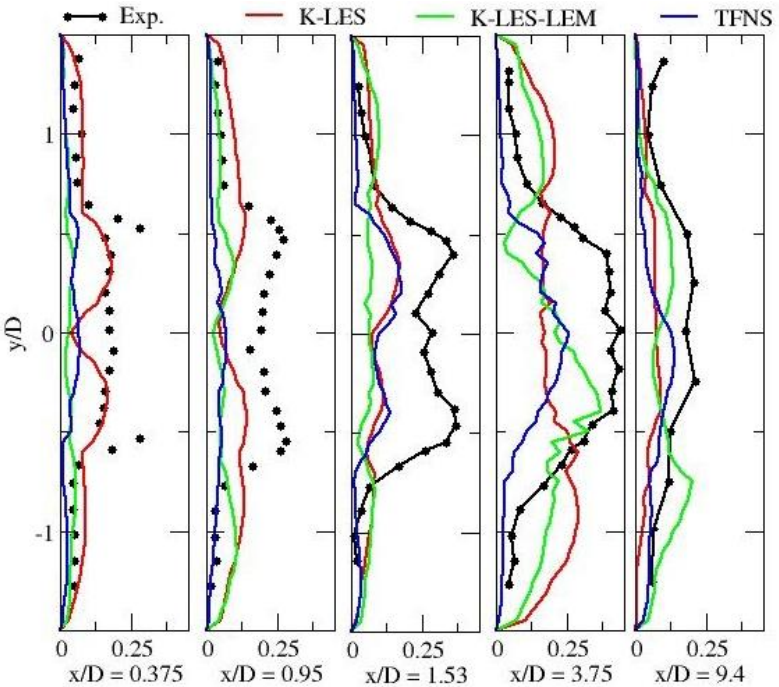

Transverse profiles of normalized RMS Y-velocity at different axial locations

Reacting case

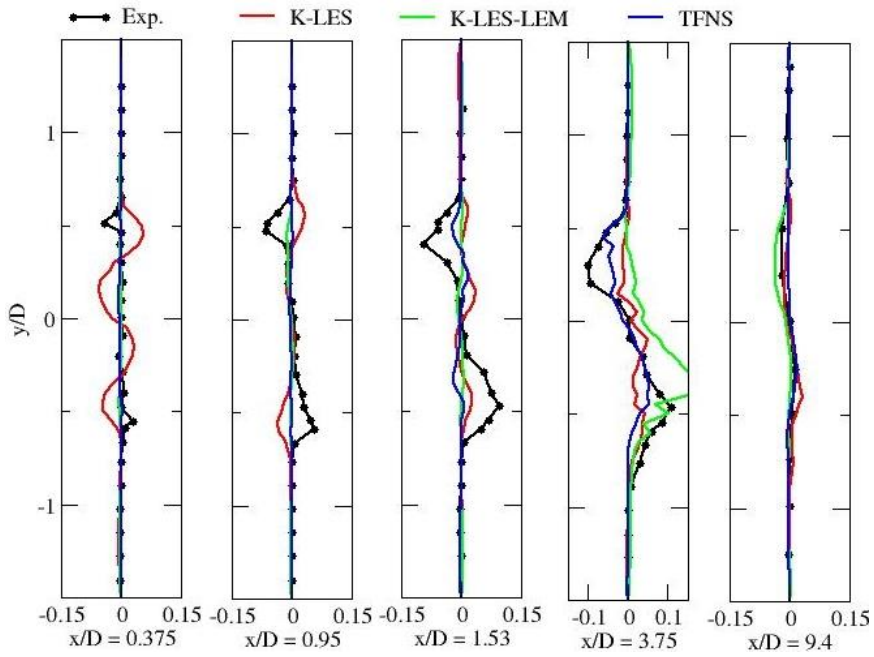

Transverse profiles of mean Reynolds stress at different axial locations from a two-step global kinetic reaction model for propane .

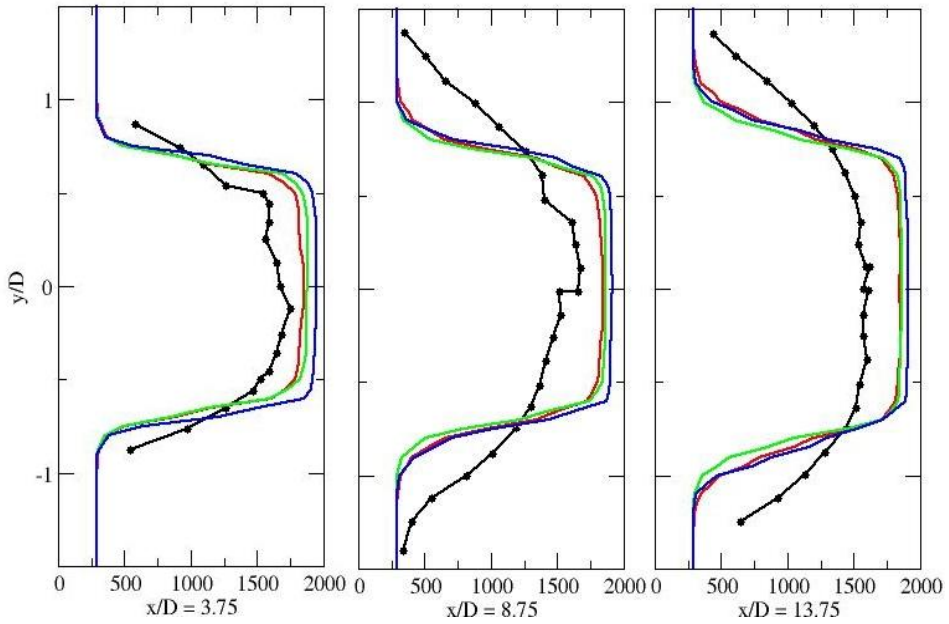

Transverse profiles of mean temperature (K) at different axial locations from a two-step global kinetic reaction model for propane .

Concluding Remarks

- A non-reacting case for the bluff-body flame holder configuration is investigated with TFNS approach on a 1600k polyhedral grid that refined from a 800k grid downloaded from the workshop webpage. The numerical solutions moderately predict the non-reacting flow field in terms of mean profiles.
- For the reacting case, the bluff-body flame holder configuration is investigated with K-LES, K-LES-LEM and TFNS approaches on the original 800k grid downloaded from the workshop webpage.
- All three reacting simulations predict that the flame is symmetric. All three reacting simulations produce time averaged axial velocities that are comparable to the experimental data in the recirculation zone.
- The time averaged Y-velocities are predicted less accurately compared to the experimental data in the recirculation zone.

Concluding Remarks

- All three reacting simulations over-predict the mean temperature due to global mechanism. All reacting turbulence fluctuations are poorly predicted due to not sufficient data saved.
- Finally, for the current work, the most important impact that determines the quality of the reacting simulations is the lack of the proper reaction kinetics.
- For the next workshop, the coding effort to store unsteady data for many specified profiles inside the CFD code is pending.

Acknowledgements

Supported by the NASA Transformational Tools and Technologies (TTT) project under the Transformative Aeronautics Concepts (TACP) program.